

Swift J0503.7–2819: A Short-Period Asynchronous Polar or Stream-Fed Intermediate Polar

J. P. HALPERN¹

¹*Department of Astronomy and Columbia Astrophysics Laboratory, Columbia University, 550 West 120th Street, New York, NY 10027-6601, USA; jph1@columbia.edu*

ABSTRACT

We analyze a 7.4 hr XMM-Newton light curve of the cataclysmic variable Swift J0503.7–2819, previously classified using optical periods as an intermediate polar (IP) with an orbital period of 0.0567 days. A photometric signal at 975 s, previously suggested to be the spin period, is not present in X-rays and is readily understood as a quasi-periodic oscillation. The X-ray light curve instead shows clear behavior of a highly asynchronous polar (AP) or stream-fed IP. It can be described by either of two scenarios: one which switches between one-pole and two-pole accretion, and another in which accretion alternates fully between two poles. The spin periods in these two models are 0.0455 days and 0.0505 days, respectively. The spin frequency ω is thus either 24% faster or 12% faster than the orbital frequency Ω , and the corresponding beat period between spin and orbit is 0.231 days or 0.462 days. Brief absorption events seen in light curve are spaced in a way that may favor the longer spin and beat periods. These periods are confirmed and refined using data from the Transiting Exoplanet Survey Satellite (TESS) and the Asteroid Terrestrial-impact Last Alert System (ATLAS). The short beat cycle of Swift J0503.7–2819 makes it well-suited to resolving this common dilemma, which amounts to deciding whether the main signal in the power spectrum is ω or $2\omega - \Omega$.

1. INTRODUCTION

Cataclysmic variables (CVs) are accreting binaries in which a dwarf star donates mass to a white dwarf (WD) via Roche-lobe overflow. X-ray surveys preferentially select CVs in which the magnetic field of the WD is strong enough to truncate the accretion disk at a magnetospheric boundary, or even prevent a disk from forming entirely. In these systems, an accretion stream is channeled onto the magnetic pole(s), where thermal plasma heated by a shock in the column just above the surface of the WD radiates X-rays. In polars (AM Her stars), the magnetic field is strong enough to channel matter directly from the companion, and the WD rotation is locked to the binary orbit. Polars are also characterized by optical circular polarization, and optical/IR humps in their spectra from cyclotron radiation in the strong magnetic field. Intermediate polars (IPs, or DQ Her stars) have weaker magnetic fields and a truncated accretion disk. The spin period of the WD in an IP is detected as a coherent oscillation in X-ray or optical emission from a rotating hot spot, at a shorter period than the orbital period of the binary.

In addition, there is a small group of “asynchronous polars” (APs), stream-fed systems in which the spin and orbit periods differ by $\leq 2\%$. The four original members of this group are V1500 Cyg, BY Cam, V1432 Aql, and CD Ind (Campbell & Schwowe 1999,

and references therein). V1500 Cyg had a nova explosion in 1975 (Stockman et al. 1988), and because it is generally observed that APs are evolving toward synchronism on a short time-scale of hundreds of years, it is believed that nova eruptions perturb the spin of the WD to create the asynchronism (Schmidt & Stockman 1991). Recently, three more members were discovered, 1RXS J083842.1–282723 (Halpern et al. 2017; Rea et al. 2017), IGR J19552+0043 (Tovmassian et al. 2017), and SDSS J084617.11+245344.1 (Littlefield et al. 2022), but they are asynchronous by 3–4%. Finally, the peculiar object RX J0524+42, also known as Paloma (Schwarz et al. 2007; Joshi et al. 2016; Littlefield et al. 2022), has been added to this group. Its spin period is 13% shorter than its orbital period. The more extreme APs may be better described as either pre-polars approaching synchronism for the first time, or stream-fed or diskless IPs if their periods are in stable equilibrium.

The subject of this Paper is the hard X-ray selected CV Swift J0503.7–2819, which we (Halpern & Thorstensen 2015) identified from the Neil Gehrels Swift Observatory BAT survey. Its Gaia-CRF3 position is R.A.=05^h03^m49^s.260, decl.=−28°23′07″.96 (Brown et al. 2021), which is referenced for proper motion to epoch 2016.0. Proper motion components are $(\mu_\alpha \cos \delta, \mu_\delta) = (+5.02 \pm 0.07, +21.87 \pm 0.08)$ mas yr^{−1}. Its parallax is 1.142 ± 0.086 mas, corresponding to

a distance of 837 (794–897) pc using geometric priors (Bailer-Jones et al. 2021). Its X-ray luminosity is 3.6×10^{32} erg s $^{-1}$ in the 0.2–12 keV band from XMM-Newton (Webb et al. 2020), and 2.4×10^{32} erg s $^{-1}$ in the 14–195 keV Swift BAT survey band¹.

In Halpern & Thorstensen (2015) we measured an orbital period of 0.0567 days in Swift J0503.7–2819, both from radial velocity spectroscopy and time-series photometry. We interpreted another photometric signal at 975 s as a spin period, which would make Swift J0503.7–2819 a rare example of an IP below the 2–3 hr (orbital) period gap in CVs. Here, we present an analysis of an archival X-ray observation (Section 2) that does not show a 975 s period. Instead, it reveals two possible values for the spin period, both of these close the orbital period. As a result, classification of Swift J0503.7–2819 as an AP or a nearly synchronous stream-fed IP is preferred. The optical evidence is revisited in view of this new information in Section 3. More precise values for the periods are found in archival survey photometry. The difficulty of identifying the correct spin period, and the arguments for and against the presence of an accretion disk, are discussed in Section 4. Conclusions are presented in Section 5.

2. X-RAY LIGHT CURVE AND POWER SPECTRUM

Swift J0503.7–2819 was observed by XMM-Newton on 2018 March 7 (ObsID 0801780301) for 7.4 hr. We used the processed event files from the two EPIC MOS cameras and the EPIC pn cameras to create X-ray light curves. Fast-mode data were taken by the Optical Monitor in the *V* filter. Although these are too faint to be useful for timing analysis, the mean magnitude of $V = 18.1$ is consistent with historical values (see Section 3).

Figure 1 shows the light curve from the combined MOS cameras, which have 1610 s longer exposure time than the pn. The softness ratio (0.15–1.5 keV)/(1.5–10 keV) is also displayed, using both the pn and the MOS to improve the statistics. The main feature of the light curve is one that is common in polars: periodic flat dips which are each too long to be an eclipse by the secondary star or its accretion stream. They are not due to photoelectric absorption, as their softness is maintained throughout. Rather, they are caused by the WD self-occulting a hot spot near its surface. Since the emission lasts for more than half of the rotation, the spot must be in the “upper” hemisphere of the WD, i.e., closest

to the observer. However, there are additional peaks (or weakening of dips) over half of the observation that are not accounted for by a single hot spot, and may indicate emission from another location. These will be investigated with the help of a power-spectrum analysis. In addition, there are three or four shorter dips in the softness ratio, indicating a drastic drop in the soft (0.15–1.5 keV) X-rays due to photoelectric absorption.

We calculated Z_1^2 periodograms from the barycentered photon arrival times from the combined pn and MOS data in their overlapping time spans. Shown in Figure 2, the power spectra have three main peaks, but with different relative strengths in soft and hard X-rays. We tentatively adopt the periods from a combined 0.15–10 keV power spectrum and list them in Table 1. Note that the uncertainties listed in Table 1 are purely statistical, and are smaller than possible systematic effects due to the limited span of the observation with respect to the various periods found. Therefore, the precision implied by the number of digits used here should not be taken literally. More precise values found optically will be given in Section 3.

The only X-ray signal that is familiar from our optical study (Halpern & Thorstensen 2015) is the lowest frequency one, at 17.62 day $^{-1}$ (0.0567 day). It is identical within errors to the 0.0567 day optical orbital period. But this is not the period between the X-ray peaks, which is better represented by the peak at 22.23 cycles day $^{-1}$ (0.0450 day). This is one reason why we maintain that the optical period is in fact the orbital period. In order to try to explain the detailed behavior of the X-ray light curve, we next propose two possible scenarios, each involving contributions from two emitting poles. In the first model, only one of the poles is accreting continuously. In the second model, accretion switches completely between poles and the spin period has a different value from the first model.

2.1. Model 1: One-pole/two-poles

Assuming that the 22.23 cycles day $^{-1}$ (0.0450 day) peak is the spin period, the times when each of two hot spots, separated by 180° of longitude, cross the meridian, are marked in Figure 1a. The dominant spot emits continuously, but extra emission partly fills in between four consecutive pulses. If this is emission from a second pole in antiphase to the first, it means that the accretion stream switches from feeding one pole exclusively, to feeding both poles for approximately half of the beat cycle between the spin and orbit. The beat frequency $\Omega_b = \omega - \Omega$ corresponds to a period of 0.217 day, which is shorter than the length of the observation. By the sixth

¹ <https://swift.gsfc.nasa.gov/results/bs157mon/>

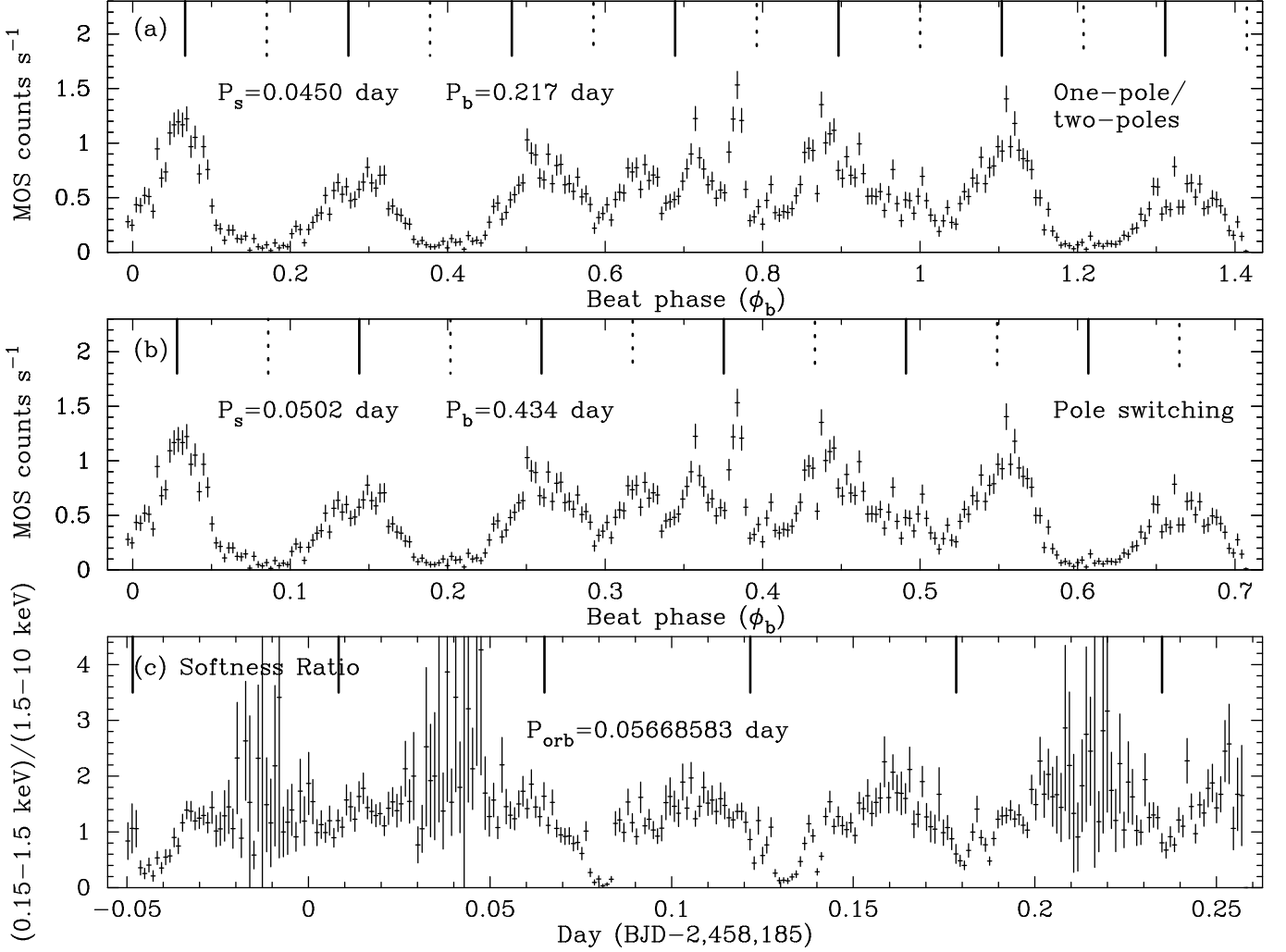


Figure 1. XMM-Newton EPIC MOS light curve (0.2–10 keV) in 100 s bins, marked with the meridian crossing times of the two accreting poles using the alternative model spin periods (P_s) from Table 1, and the orbital period. (a) Solid lines mark a dominant pole that accretes continuously. The secondary pole (dotted lines) only sometimes accretes. An entire beat period (P_b) is contained within the observation. Phase 0 of the beat cycle is arbitrary. (b) The pole-switching model requires a longer spin period, and the beat period is twice as long as above, and is not completely covered by the observation. (c) Ratio of counts in the 0.15–1.5 keV band to the 1.5–10 keV band. The EPIC pn data have been included to improve the statistics. The solid lines mark orbital phase 0 defined as the epoch of blue-to-red crossing of the optical emission-line radial velocity (see Section 3.3)

and seventh observed pulse from the dominant pole, the pattern has started to repeat and again only the dominant pole is accreting.

There are two or three sharp dips in the softness ratio beginning at day 0.082 (Figure 1c). This coincides with the time that the second pole starts accreting, and it occurs on its meridian crossing. It is possible that this represents absorption by the newly fed stream accreting onto the second pole, enabled by its particular geometry. e.g., if it is in the lower hemisphere. The absorption at this phase then weakens for each successive rotation. Finally the second pole stops accreting, and only the dominant pole emits. However, the spacing between the

absorption dips is slightly longer than the spin period, and it is not clear what the role is of a possible dip at the very beginning of the observation, on day –0.045.

The effects of the absorption on the power spectra are dramatic. In soft X-rays, emission from the second pole is suppressed, while the dominant pole continues to accrete. With little evidence in soft X-rays that there is another pole, the beating effect is weak and the orbital frequency is suppressed in the power spectrum. In the hard X-rays, the feeding of the second pole flattens the spin modulation and creates power at the beat frequency. This in turn creates sidebands of the spin signal at $\omega \pm \Omega_b = \Omega$ and $2\omega - \Omega$. The Ω (lower) sideband is

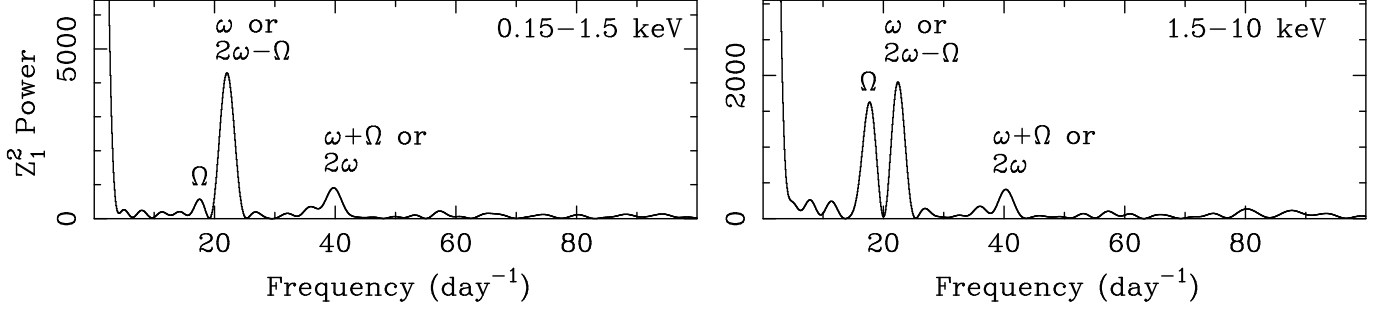


Figure 2. Periodograms of the combined pn and MOS data for the soft (0.15–1.5 keV) and hard (1.5–10 keV) X-rays. A periodogram of the total energy range was used to measure the frequencies listed in Table 1. Alternative identifications of two of the three marked peaks are indicated. These alternatives define models 1 and 2. The identification of the orbital frequency Ω is unambiguous and is used for both models in Table 1.

Table 1. X-ray Observed and Inferred Frequencies

Frequency (day ⁻¹)	Period (day)	Model 1 (One-pole/two-poles)	Model 2 (Pole switching)
17.62(4)	0.0567	Ω	Ω
22.23(3)	0.0450	ω	$2\omega - \Omega$
39.97(7)	0.0250	$\omega + \Omega$	2ω
19.93	0.0502	...	ω
4.61	0.217	$\omega - \Omega$...
2.31	0.434	...	$\omega - \Omega$

NOTE—Frequencies above the line are the three observed in the periodogram (Figure 2); those below the line are inferred.

prominent in hard X-rays, while the upper sideband is present, but very weak. It is not clear what produces this asymmetry. Perhaps it is the short observation not being commensurate with the beat period. There are also an uncertain number of narrow flares that complicate any simple picture.

The third-highest peak in the power spectrum, at a frequency of 39.97 day^{-1} (0.0250 day), is consistent with being the sum of the first two, namely $\omega + \Omega$. But is not clear what would produce it. It is natural to get $|\omega - \Omega|$ if a single pole is accreting. But to get $\omega + \Omega$ would require either retrograde spin, or pole-switching with asymmetric poles (Wynn & King 1992).

2.2. Model 2: Pole switching

A different description of the power spectrum is commonly considered for APs that show evidence for complete pole-switching, that is, when only one pole accretes at a time. This was first described by Wynn & King (1992) in the context of IPs, but is applied frequently to APs (see Wang et al. 2020, Littlefield et al. 2022, and references therein). If the poles are diametrically opposed but both visible, then the light curve consists of

alternating segments, each modulated at the spin period, but phase-shifted by 180° . The effect on the power spectrum is to drastically weaken the spin signal ω , replacing it with the two sidebands at $\omega \pm \Omega_b = \Omega$ and $2\omega - \Omega$. This differs from model 1, in which ω has a different value and remains strong in the power spectrum.

In model 2, we identify the two strongest peaks in the power spectrum of the hard X-rays with these two sidebands, $\Omega = 17.62 \text{ day}^{-1}$ and $2\omega - \Omega = 22.23 \text{ day}^{-1}$. The identification of Ω is therefore unchanged, while the now unseen spin frequency is inferred to be 19.93 day^{-1} (0.0502 days), midway between the two peaks. The beat period is $(\omega - \Omega)^{-1} = 0.434$ days, twice the length of the beat period in model 1. Therefore, the observation did not cover the entire beat cycle in this model.

There is an interval when both poles accrete, between day 0.07 and 0.19 in Figure 1 when the switch is slowly taking place. The third peak in the power spectrum, now identified with 2ω , would come from this interval. Before and after that there is clearly only one pole visible because the flux goes almost to zero between pulses. A different pole accretes at the end of the observation than at the beginning. In an antipodal geometry in which the flux from each pole goes to zero during its occultation by the WD, the sum of the observer’s viewing angle i from the spin axis and the magnetic dipole inclination m , must be $> 90^\circ$. In addition, for the length of the occultation of the two spots to be nearly the same, as seems to be the case, the angle i should be large, but not so close to 90° as to allow eclipses of the white dwarf by the secondary. No such solid-body eclipses are seen.

In the idealized model with no photoelectric absorption, the sidebands Ω and $2\omega - \Omega$ have the same strength (Wynn & King 1992; Wang et al. 2020), which is approximately the case for the hard (1.5–10 keV) X-rays in Figure 2. For the soft (0.15–1.5 keV) X-rays, the Ω sideband is reduced by photoelectric absorption suppressing some of the emission from the second pole, as

indicated by the dips in the softness ratio during the pole-switching interval.

What about the location of the absorption dips in this model? Here they come midway between the peaks of the accreting poles, that is, when the poles are at quadrature phase in their rotation and both are accreting. If we envision a switching accretion stream stretching out to reach a new pole, then it does seem possible that the stream will be viewed along its length at the limb of the WD, and occult that pole as it rises. The spacing between the dips is more compatible with the spin period of model 2 than model 1, although this is somewhat ambiguous because there is substructure in the dips. But the spacing is certainly incompatible with the orbital period. Interestingly, the possible additional dip at day -0.045 can be understood as coming 2.5 rotation periods before the next dip at day 0.082. This could mean that it is the last occurring absorption event from the other pole. If so, these dips favor model 2, since they are evidence for the existence of the other half of the hypothesized 0.434 day beat cycle.

3. OPTICAL EVIDENCE

3.1. MDM Observatory (2013 December–2014 January)

Halpern & Thorstensen (2015) reported a spectroscopic orbital period of 0.05662(9) day from emission lines, primarily He I and He II, and a consistent period of 0.05667(5) day from time-series optical photometry in a broad-band GG420 filter. However, the strongest photometric signal was at the harmonic, 0.028345(12) day. Figure 3a shows the periodogram of the time series from that study. The inset shows the light curve folded on the orbital period. In addition to the orbital frequency Ω and its harmonic 2Ω , a possible detection of a signal corresponding to either the spin frequency ω or $2\omega - \Omega$ from the X-rays is marked. Like the other signals, it is aliased by the daily sampling. A peak at 21.98 day^{-1} is the one that is closest to the X-ray value of 22.23 day^{-1} .

Power around 88 cycles day^{-1} , previously attributed to a spin period, is apparently a quasi-periodic oscillation (QPO). This is clear because (1) it is not present in X-rays, (2) its power is more broadly distributed in frequency than the other signals in Figure 3a, and (3) its origin can be deduced from the optical light curves in Halpern & Thorstensen (2015), where short series of intense but intermittent flares with the appropriate spacing are seen. These may be of the same origin as fast flares in the X-ray light curve near day 0.11 in Figure 1. Such $\approx 1000 \text{ s}$ QPOs are common in CVs, and Warner (2004) relates them to the rotation period of vertically

extended structures in the outer disk both reflecting and obscuring the central source.

3.2. TESS (2020 November 20–December 16)

A 120 s cadence light curve of Swift J0503.7–2819 was obtained by the Transiting Exoplanet Survey Satellite (TESS; Ricker et al. 2015), spanning 26 days starting on 2020 November 20. We downloaded the processed light curve and used it to calculate the periodogram in Figure 3b. It shows the same features as the MDM and XMM-Newton data, but with much greater precision, and free of aliases. Notably, the ω or $2\omega - \Omega$ signal is clearly detected at 21.971 day^{-1} , as is a weaker signal at 13.308 day^{-1} . The latter is either $2\Omega - \omega$ or $3\Omega - 2\omega$. It was also possibly present in the MDM power spectrum among several aliases. The light curve folded on Ω looks much the same as the earlier MDM one, but there is less power in the harmonic than in the fundamental.

We consider that the frequencies measured by TESS (and also ATLAS, see below) are consistent with the ones from XMM-Newton and should supplant them, considering the systematic effects that must plague the short X-ray observation. Table 2 lists the optically determined values and their identifications with the model frequencies. Subsequent discussion adopts these values.

3.3. ATLAS (2015 October–2022 January)

We downloaded photometry of Swift J0503.7–2819 from the Asteroid Terrestrial-impact Last Alert System (ATLAS; Tonry et al. 2018) forced photometry server, which is useful for confirming and extending the record of the optical behavior of Swift J0503.7–2819. After filtering out points with uncertainties $> 0.2 \text{ mag}$, there are 1148 observations in the “orange” o filter (560–820 nm) spanning 2300 days between 2015 October and 2022 January. The mean magnitude is fairly constant during this entire period at $o = 17.97$, which is similar to the GG420 magnitude calibrated approximately as $o = 17.75$ in the MDM light curve, and $V = 18.1$ in the XMM-Newton OM. A periodogram of the ATLAS data (Figure 3c) shows the same orbital period as the MDM data, but it is much more precise because of the long time span. The period is 0.05668583(14) days. The folded light curve looks much the same as the ones from MDM and TESS. The weaker signals involving the spin (not shown in Figure 3c) are also listed in Table 2.

The high precision of the ATLAS period enables us to establish the phase of all of the folded light curves in Figure 3 with respect to the MDM radial velocity curve, even though the MDM observations were obtained ≈ 620 days before the start of ATLAS. The light curves are folded on the ATLAS period, with

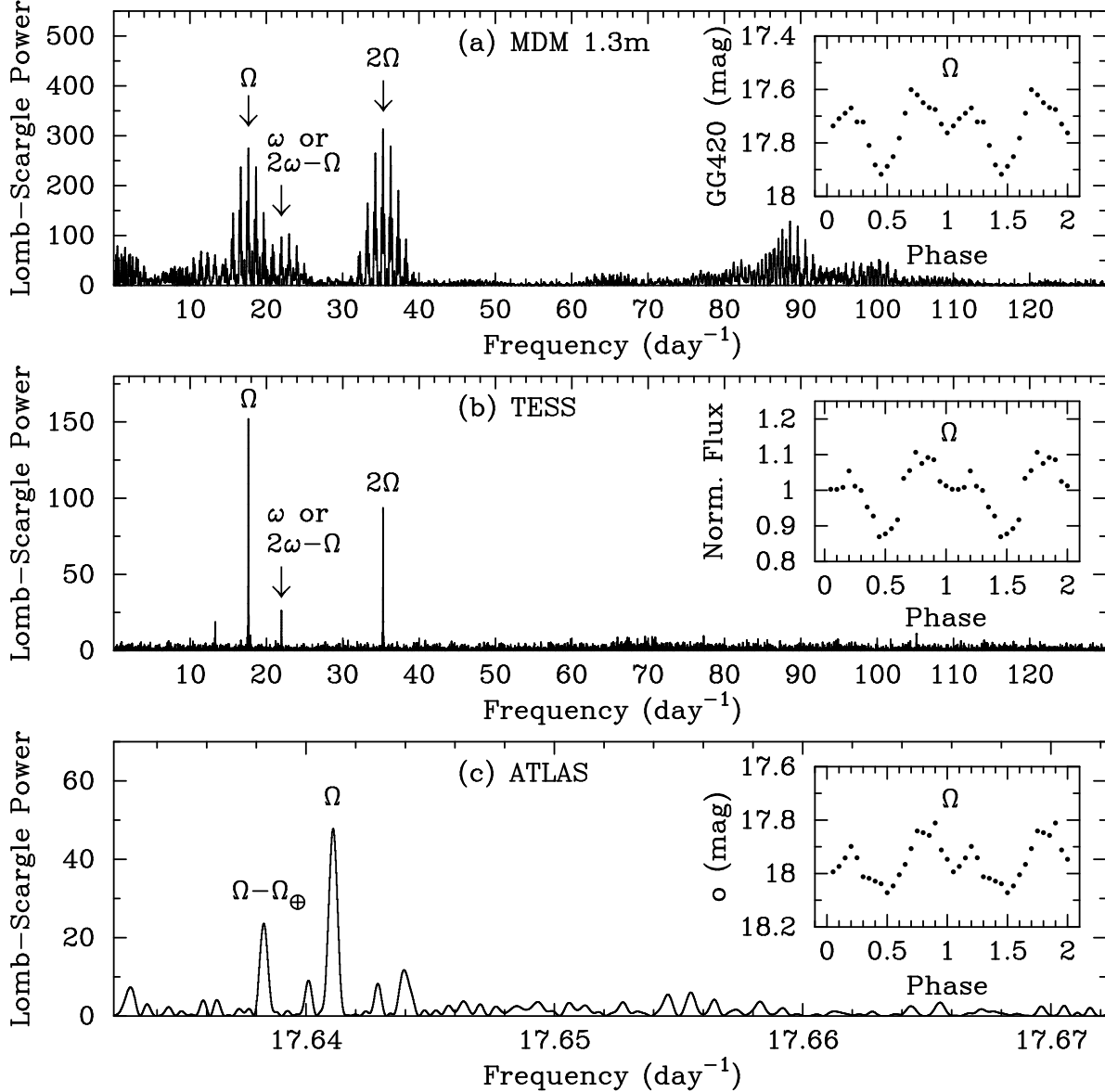


Figure 3. (a) The periodogram of the optical time-series photometry of Swift J0503.7–2819 from Halpern & Thorstensen (2015). The orbital frequency Ω is consistent with the emission-line radial velocity value in the same study. Power centered around 88 cycles day⁻¹ is now attributed to a QPO. (b) The periodogram from TESS finds the same signals as MDM and XMM-Newton but with higher precision. (c) The periodogram of the ATLAS *o* filter photometry from 2015–2022 shows the orbital frequency with yet higher precision. The second-highest peak is a 1 yr alias of Ω . In all panels the insets are the light curves folded on the ATLAS orbital period and repeated once. Phase 0 is the epoch of blue-to-red crossing of the emission-line radial velocity (see Section 3.3).

phase 0 corresponding to the blue-to-red crossing of the emission-line radial velocity, at BJD 2,456,683.6274(9) (Halpern & Thorstensen 2015). The same ephemeris is also applied to the 2018 XMM-Newton light curve in Figure 1c.

3.4. Interpretation

Now that we are considering an interpretation as an AP, there is ambiguity in interpreting an optical pe-

riod that potentially arises from emission in an accretion stream. The stream leaves the secondary star and ends on the WD, which are rotating at different frequencies. If there is pole switching, the stream has to break and reform at a different location, causing phase jumps. Furthermore, the emission-line source may not be at the location of the optical continuum that modulates the broad-band photometry, the latter being cyclotron radiation from low in the accretion column, while the optical lines are emitted higher up. Unlike in a synchronous po-

Table 2. Optical Observed and Inferred Frequencies

Frequency (day ⁻¹)	Period (day)	Model 1	Model 2
TESS			
13.3085(55)	0.075140(31)	$2\Omega - \omega$	$3\Omega - 2\omega$
17.6395(20)	0.056691(6)	Ω	Ω
21.9717(57)	0.045513(12)	ω	$2\omega - \Omega$
35.2820(27)	0.028343(2)	2Ω	2Ω
ATLAS			
13.30867(7)	0.0751390(4)	$2\Omega - \omega$	$3\Omega - 2\omega$
17.641093(44)	0.05668583(14)	Ω	Ω
21.97355(12)	0.04550927(25)	ω	$2\omega - \Omega$
35.282186(80)	0.028342915(64)	2Ω	2Ω
Inferred			
19.80732(6)	0.0504864(17)	...	ω
4.33242(8)	0.230818(4)	$\omega - \Omega$...
2.16621(4)	0.461636(9)	...	$\omega - \Omega$

lar, the accretion stream in an AP can reach a long way around the WD (see references in [Littlefield et al. 2015](#)). The emission lines can also have contributions from the ballistic accretion stream and the heated face of the secondary. Therefore, it is not obvious whether the optical emission should be tied to the rotating frame of the WD or the orbital frame of the secondary.

In the case of Swift J0503.7–2819, it is likely that the 0.0567 day period is the orbital period because it disagrees with either of the two candidates for the X-ray pulse period, which is most naturally the spin. We also checked specifically for evidence of the X-ray spin period candidates in the radial velocity data, including if they had been suppressed by pole switching, but found no indication that pole switching had affected the radial velocities, and therefore no evidence for the spin period itself.

If the emission-line velocities are orbital, they are too broad to be coming from the heated face of the secondary, while [Halpern & Thorstensen \(2015\)](#) state that they do not show the asymmetric, shifting wings typical of a polar. Therefore, it is possible that they come from an accretion disk. The radial velocity amplitude of $189 \pm 20 \text{ km s}^{-1}$ is larger than that of most IPs, but smaller than that of most polars. There are also two potential sources of optical continuum light: the disk, and a stream that manages to pass over the disk and accrete directly onto a magnetic pole. A stream is necessary in order to make the WD poles aware of the orbital pe-

riod, evident in the X-ray power spectrum, information which they would not have in the case of a conventional disk-fed IP.

Note also that optical emission lines from accretion disks generally do not represent the orbital velocity of the compact object, which in this case should be $\approx 60 \text{ km s}^{-1}$ assuming a $0.8 M_{\odot}$ WD with a $0.1 M_{\odot}$ secondary star. Rather, their velocities are due to asymmetric features in the fast-rotating disk. Therefore, they are an unreliable indicator of orbital phase even while they reveal the orbital period. This complicates any interpretation of the folded optical light curve in Figure 3 that attempts to relate it to spectroscopic phase.

Without knowing the absolute orbital phase, the double-peaked shape of the folded optical light curve in Figure 3 is open to more than one interpretation, but none is highly satisfactory. The first could involve primary and secondary eclipses, but the main broad dip is too wide to be an eclipse. Second, it could represent a combination of ellipsoidal modulation and heating of the inner face of the secondary by the X-ray source. The heating contributes most at the fundamental frequency, while the ellipsoidal modulation is responsible for the harmonic. However, the strong optical flickering and, more importantly, absence of photospheric absorption lines in the spectrum, do not allow for a major contribution of the secondary’s photosphere to the optical light, while in this interpretation the photosphere must contribute at least 30%.

Third, the double peaks could represent emission from a more elongated, optically thick accretion funnel or stream coming off the secondary, which has a larger projected area as seen from the side. This is often invoked for accretion columns in general, but ones that are attached to the spinning frame, not the orbiting frame that we are restricted to here. This is essentially a more extreme version of the second proposal, but removed from the stellar photosphere and also not attached to the WD. Finally, it may just be easiest for a disk to reveal the orbital signature in optical light, as it directly taps the majority of the available gravitational potential energy, and may have persistent asymmetry driven by accretion from the secondary.

4. DISCUSSION

The basic properties of nearly all APs are difficult to determine because it is not certain which periods represent the spin and the orbit. It is most helpful if at least the orbital period can be identified unambiguously by a radial velocity curve of photospheric absorption lines on the secondary, but these are often not detectable, including in Swift J0503.7–2819. Instead, we have a

fairly secure but not ironclad case for Ω as the optical emission-line and photometric period. A very precise period derived from 6.3 yr of ATLAS photometry allows the optical light curves, radial velocity curve, and X-ray light curve to be aligned in phase. How this corresponds to the absolute phase of the binary orbit remains an open question.

The spin period can in principle be measured from a segment of the X-ray light curve between pole switches as we did for 1RXS J083842.1–282723 (Halpern et al. 2017), an analysis that benefits from strong and regular pulse shapes. However, even in such clear cases there is the complication that the footpoint of the accretion column is not expected to be fixed on the surface of a WD in an AP (Geckeler & Staubert 1997). Seen from a fixed point on the WD, the secondary orbits in the retrograde direction if $\omega > \Omega$. As the secondary transits over a pole, the accreting matter is captured and threaded onto different field lines. The result is seen clearly as a spin-phase drift during every beat cycle (Littlefield et al. 2019, 2022), although it is not clear if the model of Geckeler & Staubert (1997) correctly describes the result in all APs (Littlefield et al. 2019). Such an effect would be difficult to recognize and quantify in an X-ray observation that covers less than a full beat cycle, as was likely the case here and for 1RXS J083842.1–282723.

Switching of the accretion between poles changes the peaks in the power spectrum; this must be recognized if the periods and accretion geometry are to be correctly identified. The spin period is often not present in the power spectrum if there is pole switching, which can make the dominant peak either $\omega - \Omega$ if $i + m$ is small, or split ω into the sidebands Ω and $2\omega - \Omega$ if $i + m$ is large (Wynn & King 1992; Wang et al. 2020). In addition to the identifications of ω and Ω possibly being reversed, an ambiguity for an AP is whether to identify the upper sideband as ω (model 1) or $2\omega - \Omega$ (model 2). See, e.g., Myers et al. (2017), Littlefield et al. (2019), and Wang et al. (2020) on CD Ind. It was even inferred that accretion in CD Ind and Paloma switched from single- to two-pole around the beat cycle (Hakala et al. 2019; Littlefield et al. 2022), much like our model 1.

The alternative identifications of the main peak in the X-ray power spectrum of Swift J0503.7–2819 come with a beat period differing by a factor of 2, which means that the observation either spans more than one beat period (model 1) or less than one beat period (model 2), with slightly different spin periods to match the pulse to the correct pole. Additional evidence that may bear on which model is correct comes from the absorption dips. The second pole seems to suffer photoelectric absorption for up to three spin periods, which is most of the

time that it is accreting in model 1, but only a fraction of the time in model 2, where the second pole eventually emerges looking much like the first pole in its pulse profile. It might seem that this is too much fine tuning for model 2. On the other hand, the spacing of the absorption dips is more consistent with the spin period of model 2 than model 1. Furthermore, model 2 requires one out of the four dips to be coming from the opposite pole during the other half of the beat cycle, which lends model 2 additional support.

A longer X-ray observation would likely resolve the ambiguity of the beat frequency. If model 1 is correct, a second 0.231 day cycle will look much the same as the first, while in model 2 there should be differences because a second pole will be accreting. The uncertain outcome of the present study is due to the limited length of the observation. It is even possible that the apparent change of state to two-pole accretion (or flaring) is simply a random event that will not repeat on a regular period. In that case, the simpler model 1 is probably correct as far as its period assignments are concerned. On the other hand, this supposed random event is what is responsible for the strong peak in the hard X-ray power spectrum at precisely the orbital frequency determined optically. This would be quite a coincidence.

Whether or not there is pole switching also bears on the question of whether there is an accretion disk, as hinted at by the optical emission-line properties. An X-ray signal at $2\omega - \Omega$ is a clear signature of stream-fed accretion. In a conventional IP that is fed from a truncated accretion disk, the inner disk has erased all information about the location of the secondary. So it is difficult to imagine how a 2ω spin signal could be modulated strongly at the orbital frequency Ω , which would require X-ray reflection by material fixed in the orbital frame, while suppressing the underlying spin signal. If model 1 is correct *and* the apparent beat-induced episode is not random, the same objection applies, in the sense that the inner accretion disk “knows” when to contribute to the second pole. Interestingly, the optical power spectra do have signals involving the spin frequency, albeit weaker than the ones at Ω and 2Ω . These could be from a contribution to the optical light from accretion columns, or a reprocessing of the X-ray spin pulses on the secondary.

5. CONCLUSIONS

Using an archival XMM-Newton observation, we identified candidates for the spin frequency of Swift J0503.7–2819 that are either 24% or 12% faster than the orbital frequency determined optically. We then refined their values using TESS and ATLAS pho-

tometry. Either value of the frequency excess is characteristic of a small class of highly asynchronous polars or stream-fed IPs. The ambiguity arises because it is not clear if a complete pole-switching event took place during the observation. If it did, it requires assigning $2\omega - \Omega$ to the main peak in the power spectrum instead of ω in the case of single-pole accretion. Absorption dips in the light curve tend to support $2\omega - \Omega$, therefore 12% asynchronism. The most important follow-up to resolve this question would be a longer X-ray observation that covers at least a full cycle or two of the longer 0.462 day beat candidate. This should reveal whether a different pole is alternating in accretion with the first, through inevitable differences in viewing geometry, obscuration, or size. A similar AP that has not yet been observed through its suggested 44 hr beat cycle is 1RXS J083842.1–282723 (Halpern et al. 2017).

The optical emission lines of Swift J0503.7–2819 do not display the properties common in ordinary polars, particularly the high velocities of the latter from radial accretion. While radial velocities are generally expected to be modulated on the spin period if they come from deep in the accretion column, this appears not to be the case in several APs, including Swift J0503.7–2819, 1RXS J083842.1–282723, and IGR J19552+0043 (Tovmassian et al. 2017), in which they represent the orbital period. They may have to come from an accretion disk, or from extended streams that wrap around the WD to reach the magnetic poles. The optical QPO of Swift J0503.7–2819 is also a characteristic of disk systems.

If there is a disk present, there must also be a stream that jumps over the disk to directly feed the magnetic poles, i.e., the disk-overflow model of IPs (Hellier 1993). Otherwise, the beating effect would be difficult to understand. As to whether Swift J0503.7–2819 is a pre-polar approaching synchro-

nism, or an equilibrium IP, the magnetic accretion model of Norton et al. (2004) predicts that rotational equilibrium should only be possible when $P_s/P_{\text{orb}} < 0.6$, which means that Swift J0503.7–2819 should be in the process of synchronizing. Indeed, the candidates for nearly synchronous IPs listed in Norton et al. (2004) with $P_s/P_{\text{orb}} > 0.7$ have subsequently been judged instead to be already synchronous polars², with the exception of Paloma, the AP that Swift J0503.7–2819 most closely resembles.

I thank the anonymous referee for recommending several improvements, and offering generous advice, including finding evidence in TESS and ATLAS data. Slavko Bogdanov provided assistance with the XMM-Newton OM data. John Thorstensen and Colin Littlefield obliged me with helpful discussions. Joe Patterson warned me years ago that the 975 s signal is probably a QPO.

This work was supported by NASA grant 80NSSC21K0819, and is based on observations obtained with XMM-Newton, an ESA science mission with instruments and contributions directly funded by ESA Member States and NASA. This paper includes data collected with the TESS mission, obtained from the MAST data archive at the Space Telescope Science Institute (STScI). Funding for the TESS mission is provided by the NASA Explorer Program. The ATLAS project is primarily funded to search for near earth asteroids through NASA grants NN12AR55G, 80NSSC18K0284, and 80NSSC18K1575. The ATLAS science products have been made possible through the contributions of the University of Hawaii Institute for Astronomy, the Queen’s University Belfast, the Space Telescope Science Institute, the South African Astronomical Observatory, and The Millennium Institute of Astrophysics (MAS), Chile.

Facility: XMM, MDM, TESS, ATLAS

REFERENCES

- Bailer-Jones, C. A. L., Rybizki, J., Fouesneau, M., Demleitner, M., & Andrae, R. 2021, *A&A*, 161, 147
- Brown, A. G. A., Vallenari, A., Prusti, T., et al. 2021, *A&A*, 649, A1
- Campbell, G. C., & Schwöpe, A. D. 1999, *A&A* 343, 132
- Geckeler, R. D., & Staubert, R. 1997, *A&A*, 325, 1070
- Hakala, P., Ramsay, G., Potter, S. B., et al. 2019, *MNRAS*, 486, 2549
- Halpern, J. P., Bogdanov, S., & Thorstensen, J. R. 2017, *ApJ*, 838, 124
- Halpern, J. P., & Thorstensen, J. R. 2015, *AJ*, 150, 170
- Hellier, C. 1993, *MNRAS*, 265, L35
- Joshi, A., Pandey, J. C., Singh, K. P., & Agrawal, P. C. 2016, *ApJ*, 830, 56
- Littlefield, C., Garnavich P., Mukai, K., et al. 2019, *ApJ*, 881, 141
- Littlefield, C., Hoard, D., Garnavich P., et al. 2022, *ApJ*, in press, arXiv:220502863
- Norton, J. P., et al. 2004, *ApJ*, 612, 1000
- Tovmassian, A., et al. 2017, *ApJ*, 845, 100

² <https://asd.gsfc.nasa.gov/Koji.Mukai/iphone/iphone.html>

- Littlefield, C., Mukai, K., Mumme, R., et al. 2015, MNRAS, 449, 3107
- Myers, G., Patterson, J., de Miguel, E., et al. 2017, PASP, 129, 044204
- Norton, A. J., Wynn, G. A., & Somerscales, R. V. 2004, ApJ, 614, 349
- Rea, N., Coti Zelatti, F., Esposito, P., et al. 2017, MNRAS, 471, 2902
- Ricker, G. R., Winn, J. N., Vanderspek, R., et al. 2015, JATIS, 1, 014003
- Schmidt, G. D., & Stockman, H. S. 1991, ApJ, 371, 749
- Schwarz, R., Schwöpe, A. D., Staude, A., et al. 2007, A&A, 473, 511
- Stockman, H. S., Schmidt, G. D., & Lamb, D. Q. 1988, ApJ, 332, 282
- Tonry, J. L., Denneau, L., Heinze, A. L., et al. 2018, PASP, 130, 064505
- Tovmassian, G., González-Buitrago, D., Thorstensen, J., et al. 2017, A&A, 608, 36
- Wang, Q., Qian, S., Han, Z., et al. 2020, ApJ, 892, 38
- Warner, B. 2004, PASP, 116, 115
- Webb, N. A., Coriat, M., Traulsen, I., et al. 2020, A&A, 641, A136
- Wynn, G. A., & King, A. R. 1992, MNRAS, 255, 83

